

See discussions, stats, and author profiles for this publication at: <https://www.researchgate.net/publication/323105140>

Magnetocaloric Effect in $\text{BiFe}_{1-x}\text{Zn}_x\text{O}_3$ Multiferroics

Article in *Journal of Superconductivity and Novel Magnetism* · February 2018

DOI: 10.1007/s10948-018-4590-2

CITATIONS

4

READS

543

8 authors, including:



Abdulkarim Amirov

Immanuel Kant Baltic Federal University

47 PUBLICATIONS 213 CITATIONS

[SEE PROFILE](#)



Igor Makoed

Brest State University named after A.S. Pushkin

37 PUBLICATIONS 200 CITATIONS

[SEE PROFILE](#)



Dr. Yogesh A. Chaudhari

North Maharashtra University

18 PUBLICATIONS 81 CITATIONS

[SEE PROFILE](#)



Dibir Yusupov

Amirkhanov Institute of Physics of Daghestan Federal Research Center of Russian ...

12 PUBLICATIONS 18 CITATIONS

[SEE PROFILE](#)

Some of the authors of this publication are also working on these related projects:



Piezoelectric materials, multiferroic materials, La based chromates, manganates [View project](#)



MULTICALORIC EFFECT [View project](#)



Magnetocaloric Effect in $\text{BiFe}_{1-x}\text{Zn}_x\text{O}_3$ Multiferroics

A. A. Amirov^{1,2} · I. I. Makoed³ · Y. A. Chaudhari⁴ · S. T. Bendre⁴ · D. M. Yusupov² · A. Sh. Asvarov² · N. A. Liedienov⁵ · A. V. Pashchenko^{5,6}

Received: 21 November 2017 / Accepted: 25 January 2018
© Springer Science+Business Media, LLC, part of Springer Nature 2018

Abstract

Ceramic $\text{BiFe}_{1-x}\text{Zn}_x\text{O}_3$ multiferroic samples were prepared by the solid combustion method for $x = 0.1, 0.15,$ and 0.2 . Structural, magnetic, and magnetocaloric properties of the multiferroics have been studied. For all samples, an antiferromagnetic phase transition is observed in the region of 630 K. With increase in x , the reduction in magnitude of magnetization and Neel temperature is observed. The magnetocaloric properties, entropy, relative cooling power, and heat capacity have been calculated within the framework of thermodynamic theory. It has been established that the maximum changes of magnetocaloric properties of multiferroics are observed in the region of magnetic phase transition.

Keywords Multiferroics · Phase transitions · Magnetocaloric effect · Entropy · Relative cooling power · Heat capacity

1 Introduction

Multiferroics are the most promising materials, in which two or more types of ferroic ordering phenomena such as ferromagnetism, ferroelectricity, and ferroelasticity coexist [1, 2]. Consequently, in these multifunctional materials can exist all three types of caloric effects. In [3], the observed couple caloric effects in multiferroics were proposed to

be called as multicaloric. The first experimental results on multicaloric effects and their theoretical analysis were presented in the following works [4–11]. Nevertheless, in spite of the intensive studies of the multiferroics, the caloric effects in them are still poorly studied. This is due to the fact that a lot of the studied multiferroics have high phase transition temperatures and low magnitude of the effects, as well as they are complex objects for measuring the caloric properties in the high-temperature region due to a high error of experiment. In this connection, the use of theoretical approaches for calculation and estimation of caloric effects in the region of high-temperature phase transitions is a topical direction in both an applied aspect to search promising materials for solid-state refrigerators and a fundamental aspect to understand better the nature of interactions of the structure, magnetic, and electrical subsystems.

BiFeO_3 compounds are the best-known and well-studied multiferroics with high temperatures of phase transitions $T_N \sim 643$ K and $T_C \sim 1083$ K [12, 13]. However, existing data on the caloric effects in compounds based on bismuth ferrite are almost absent in the literature and limited by the studies on the electrocaloric effect in them [14, 15]. Thus, the problem of investigation of the magnetocaloric effect in compounds based on bismuth ferrite is topical. Particular interest presents the choice of ceramic BiFeO_3 compounds at substitution Fe ions for divalent Zn ones.

✉ A. A. Amirov
amiroff_a@mail.ru

- ¹ Center for Functionalized Magnetic Materials (FunMagMa) & Institute of Physics Mathematics and Informational Technologies, Immanuel Kant Baltic Federal University, Kaliningrad, Russia, 236016
- ² Amirkhanov Institute of Physics Daghestan Scientific Center, Russian Academy of Sciences, Makhachkala, Russia, 367003
- ³ Department of Physics, Brest State University, 224016, Brest, Belarus
- ⁴ Department of Physics, School of Physical Sciences, North Maharashtra University, Jalgaon, 425001, Maharashtra, India
- ⁵ Donetsk Institute for Physics and Engineering named after O.O. Galkin, National Academy of Sciences of Ukraine, Kyiv, 03028, Ukraine
- ⁶ Donetsk National University of Economy and Trade named after Michael Tugan-Baranovsky, Kryvyi Rih, 50005, Ukraine

2 Experiment

Ceramic $\text{BiFe}_{1-x}\text{Zn}_x\text{O}_3$ (BFZO) samples ($x = 0.1, 0.15$ and 0.2) were prepared by using solution combustion method (SCM) [16] from the precursors $\text{Bi}(\text{NO}_3)_3 \cdot 5\text{H}_2\text{O}$ (CDH, India), $\text{Fe}(\text{NO}_3)_3 \cdot 9\text{H}_2\text{O}$ (Fischer Scientific), and $\text{Zn}(\text{NO}_3)_2 \cdot 6\text{H}_2\text{O}$ (CDH, India), which were used as oxidizers, whereas glycine ($\text{NH}_2\text{CH}_2\text{COOH}$) (CDH, India) was used as a fuel. The ratios of the oxidizer and the fuel were calculated taking into account the valences of metal nitrate oxidants and glycine reducing agent, which were completely dissolved in the stoichiometric ratio. Then the mixture was heated up to the evaporation of free water and the occurrence of spontaneous combustion. The resulting BiFeO_3 powders with a different concentration of Zn were grinded and calcined at 650°C for 4 h. In these calcined powders, 2% polyvinyl alcohol was added as a binder and pellets from synthesized powders were prepared using uniaxial pressing. Lastly, the ceramics are sintered at selected temperatures depending on the Zn concentration as 675°C ($x = 0.1$), 680°C ($x = 0.15$), and 685°C ($x = 0.2$) for 30 min. The choosing of different sintering temperatures for all samples related with the strong dependence of sintering temperature from the content of impurity phases. Given this fact, each composition was chosen optimal regimes of sintering in which the formation of impurity phases is minimal. The structure of the obtained samples was studied by X-ray diffraction (XRD) method using Bruker D2 PHASER and Philips X-pert PRO diffractometers with $\text{CuK}\alpha 1$ radiation. The morphology of the ceramic surface was examined by LEO-1450 scanning electron microscope with ISYS microprobe analyzer of EDX system (Leica Microsystems Wetzlar GmbH, Germany). The Mossbauer spectra were measured by the specially designed MC1104Em spectrometer with a ^{57}Co gamma-ray source in a Cr matrix. Magnetic measurements were carried out at vibrating sample magnetometer (LakeShore 7400).

3 Results and Discussion

The surface morphology of the samples exhibits that ceramic consists of large grains ($\sim 1\ \mu\text{m}$) which are surrounded by grains with small size ($\sim 200\ \text{nm}$) (Fig. 1a). The XRD results demonstrated that the Zn-doped BiFeO_3 samples have rhombohedral perovskite structure and indicated the presence of the additional impurity phase $\text{Bi}_{12}(\text{Bi}_{0.5}\text{Fe}_{0.5})\text{O}_{19.5}$ [16]. The Mossbauer spectrum also confirms the presence of the impurity phases. For example, the Mossbauer spectra of $\text{BiFe}_{0.85}\text{Zn}_{0.15}\text{O}_3$ (Fig. 1b) are a superposition of two Zeeman sextets and two paramagnetic doublets. Doublets correspond to the iron-containing

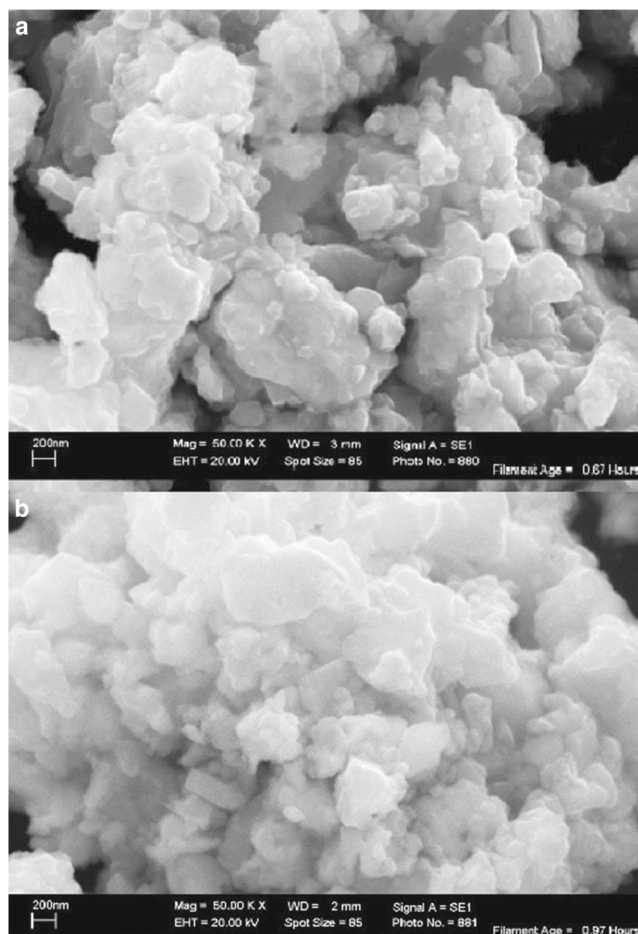


Fig. 1 Microphotographs of surface on a scanning electron microscope (SEM) for the $\text{BiFe}_{0.85}\text{Zn}_{0.15}\text{O}_3$ sample before heating (a) and after heating (b)

impurity phases, which often appear during the synthesis of BiFeO_3 (Fig. 2a) [17]. Sextets exhibit the same isomer shift corresponding Fe^{3+} in the octahedral environment, which is a typical perovskite structure, and the presence of two sextets is connected with spin cycloid structure [18].

High-temperature annealing of ceramics up to 900 K leads to the formation of recrystallization of ceramics (Fig. 1b), structural inhomogeneities, and the appearance of additional iron-containing impurity phases. All impurity phases were not identified; however, XRD spectra were detected reflexes characteristic for most commonly observed in bismuth ferrite impurity phase of iron-rich $\text{Bi}_2\text{Fe}_4\text{O}_9$ mullite (Fig. 3). The fraction of impurities arising after high-temperature annealing was not estimated.

Temperature dependences of magnetization of the $\text{BiFe}_{1-x}\text{Zn}_x\text{O}_3$ samples ($x = 0.1, 0.15$, and 0.2) in a magnetic field of 0.6 T are shown in Fig. 4. For all the studied samples in the region of 630 K is observed an anomaly, which corresponds to the temperature

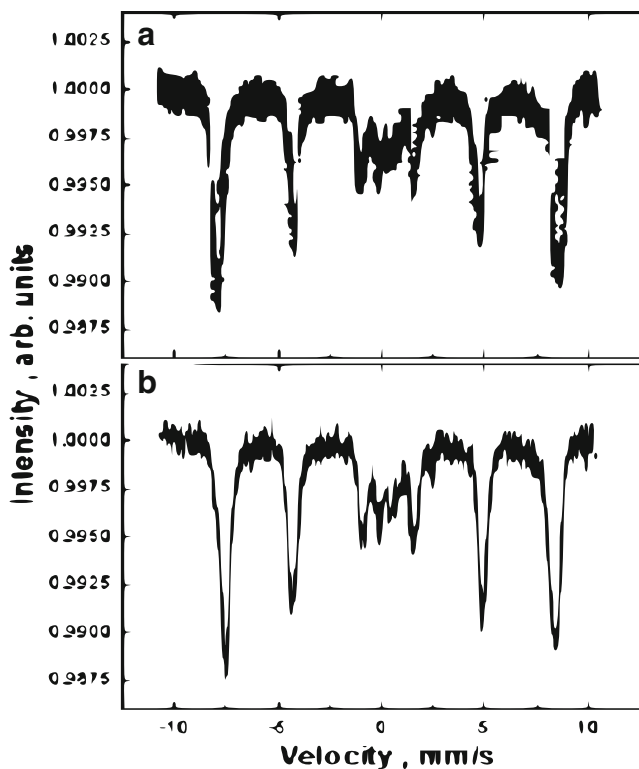


Fig. 2 Mössbauer spectra, measured for (a) BiFeO₃ and (b) BiFe_{0.85}Zn_{0.15}O₃ samples at room temperature $T = 300$ K

of antiferromagnetic transition. The observed nonzero magnetization above the antiferromagnetic transition is due to the presence of impurity magnetic phase in the samples. It should be noted that the presence of impurities and structural defects is one of the problems in the studying ceramic samples based on BiFeO₃, and their physical properties may depend on the fraction of impurity phase, density, and sintering conditions [19]. Moreover, the high temperatures also influence the initial physical parameters of the ceramics. In our case, the heating up to 900 K and cooling of the ceramics lead to irreversible

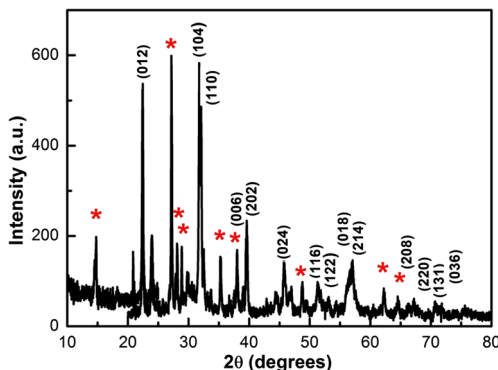


Fig. 3 XRD pattern of the BiFe_{0.85}Zn_{0.15}O₃ samples after annealing; *the peaks corresponded to the presence of the impurity phase iron rich Bi₂Fe₄O₉ mullite

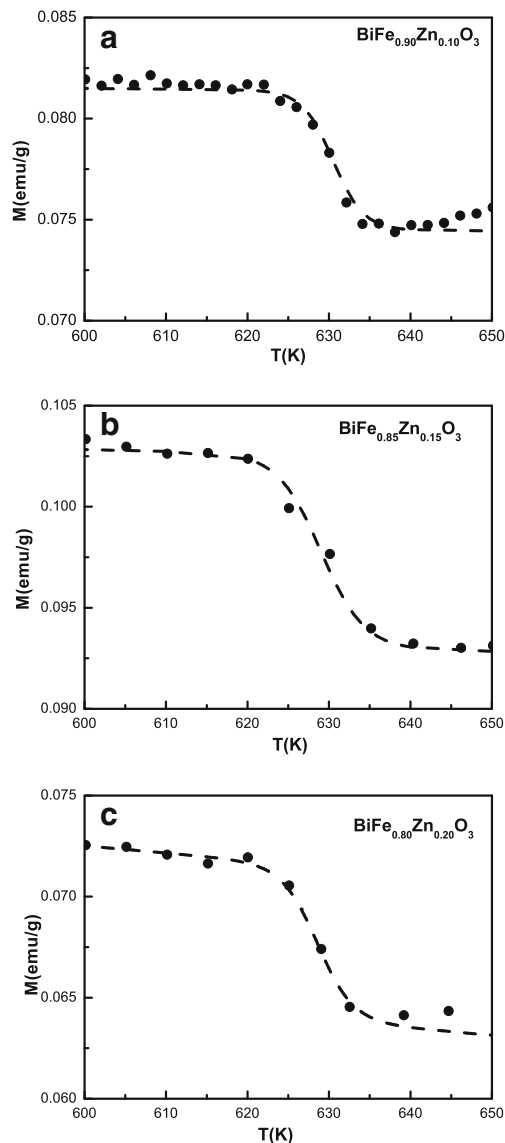


Fig. 4 Temperature dependences of magnetization for the BiFe_{1-x}Zn_xO₃ samples ($x = 0.1$ (a), $x = 0.15$ (b), $x = 0.2$ (c)) in a magnetic field of 0.6 T (points are experiment and dashed line is result of calculations)

structural changes associated with the recrystallization of the material and possible formation of a new magnetic phase (Fig. 1b). In particular, for a sample with $x = 0.15$, X-ray diffraction analysis of the structure the formation of iron-containing impurity magnetic phase due to heat treatment (Fig. 3) was confirmed. Thus, using the results of structural and magnetic investigations, it was shown that the study of magnetic and magnetocaloric properties in the high-temperature region has difficulties due to an instability of the structural and magnetic parameters. Taking into account this problem, we have proposed to describe the magnetocaloric properties in the region of magnetic transition in terms of numerical calculations, which were successfully realized in the following works [20–22].

Table 1 Parameters of model for the BiFe_{1-x}Zn_xO₃ ceramic samples in a magnetic field of 6 T

<i>x</i>	<i>M_i</i> (emu/g)	<i>M_f</i> (emu/g)	<i>T_N</i> (K)	<i>B</i> (10 ⁻⁶ emu/g*K)	<i>S_N</i> (10 ⁻⁴ emu/g*K)
0.10	0.0814	0.0745	631	- 3.03	- 9.29
0.15	0.1026	0.093	629	- 7.82	- 9.18
0.20	0.0715	0.0639	629	- 3.55	- 9.06

As known, within the framework of thermodynamic theory, the change in magnetic entropy under the influence of an external magnetic field from 0 to *H_{max}* is described by the expression:

$$\Delta S_M = \int_0^{H_{max}} \left(\frac{\partial S}{\partial H} \right)_T dH. \tag{1}$$

Using the Maxwell relation:

$$\left(\frac{\partial M}{\partial T} \right)_H = \left(\frac{\partial S}{\partial H} \right)_T, \tag{2}$$

Formulae (1) can be written in the form:

$$\Delta S_M = \int_0^{H_{max}} \left(\frac{\partial M}{\partial T} \right)_H dH. \tag{3}$$

The calculation of the temperature dependences of magnetization and magnetic entropy of the BiFe_{1-x}Zn_xO₃ multiferroics was performed by using the phenomenological model which was described and tested in the following works [20, 22]. According to [20], the temperature dependence of magnetization in the vicinity of Neel point can be described by the following expression:

$$M = \frac{M_i - M_f}{2} \tanh[A(T_N - T)] + BT + C, \tag{4}$$

where *M_i* and *M_f* are the start and end points of the temperature range of antiferromagnetic transition which were chosen so that the magnitude of deviation between the theoretical calculations and the experimental data did not exceed the error of the experiment. The value of *A* is defined as:

$$A = \frac{2(B - S_N)}{M_i - M_f}, \quad \text{where } B = \left(\frac{dM}{dT} \right)_{T_i}, \tag{5}$$

$$S_N = \left(\frac{dM}{dT} \right)_{T_N}, \tag{6}$$

$$C = \frac{M_i + M_f}{2} - BT_N. \tag{7}$$

The temperature dependences of the experimental and calculated values of magnetization for the investigated samples are shown in Fig. 4, which are in good agreement with each other. The calculated parameters of the model for the BFZO samples in a magnetic field of 6 T are listed in Table 1. The magnetic contribution to the ΔS_M entropy

varies depending on the value of the external field, which changes from 0 to *H_{max}*:

$$\Delta S_M = \left\{ -A \left(\frac{M_i - M_f}{2} \right) \operatorname{sech}^2 [A(T_N - T)] + B \right\} H_{max}. \tag{8}$$

The calculated values of ΔS_M as a function of temperature (Fig. 5) were obtained from the initial experimental parameters of magnetization. For compositions with *x*=0.15 and *x*=0.2, a similar behavior of ΔS_M is observed, which is related to the close temperatures of antiferromagnetic transition. The maximum value of the ΔS_M contribution is reached at *T* = *T_N* and defined as:

$$\Delta S_{max} = \left\{ -A \left(\frac{M_i - M_f}{2} \right) + B \right\} H_{max}. \tag{9}$$

The full width at half maximum of the peak δT_{FWHM} is determined from the expression:

$$\delta T_{FWHM} = \frac{2}{A} \operatorname{sech} \left[\sqrt{\frac{2A(M_i - M_f)}{A(M_i - M_f) + 2B}} \right]. \tag{10}$$

The evaluation of magnetic cooling efficiency, taking into account a magnitude of the change in the magnetic entropy and its width at half height, was estimated from the values of the relative cooling power (RCP) [23]:

$$RCP = -\Delta S_M(T, H_{max}) \times \delta T_{FWHM}. \tag{11}$$

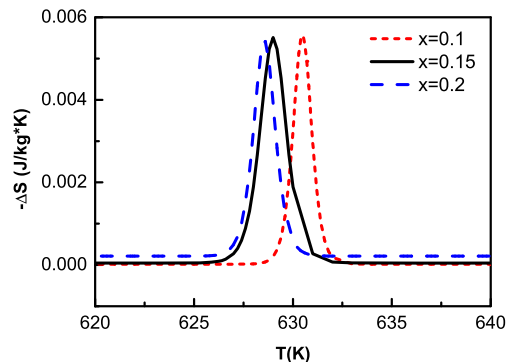


Fig. 5 Calculated values of ΔS_M entropy as a function of temperature, obtained from the initial experimental parameters of magnetization of the BiFe_{1-x}Zn_xO₃ ceramics

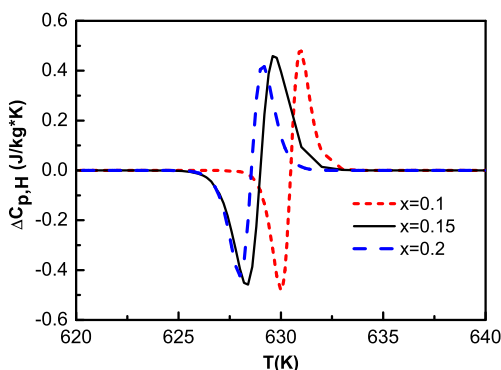


Fig. 6 Temperature dependences of calculated values of the relative change in magnetic part of heat capacity for the $\text{BiFe}_{1-x}\text{Zn}_x\text{O}_3$ ceramic samples in a magnetic field of 6 T

The change in the magnetic part of specific heat capacity was calculated by using the following expression [24]:

$$\Delta C_{p,H} = -2TA^2 \left(\frac{M_i - M_f}{2} \right) \text{sech}^2[A(T_N - T)] \times \tanh[A(T_N - T)]H_{\max}. \quad (12)$$

The temperature dependences of calculated values of the change in the magnetic part of heat capacity and RCP are shown in Figs. 6 and 7. The values of RCP are expected to be small as it follows from the data on magnetization and entropy changes. The magnetic heat capacity demonstrates typical behavior for magnetic materials. All data were obtained at $H_{\max} = 6.0$ T.

The concentration dependences of the main magnetic characteristics are listed in Table 2. The evaluation of their absolute values in an external magnetic field $H_{\max} = 6$ T indicates that these materials are hardly suitable for practical use. It should be noted that the certain correlations in behavior of these values, depending on the degree of substitution, are established. On the average, neglecting the insignificant deviations of values from nonmonotonicity,

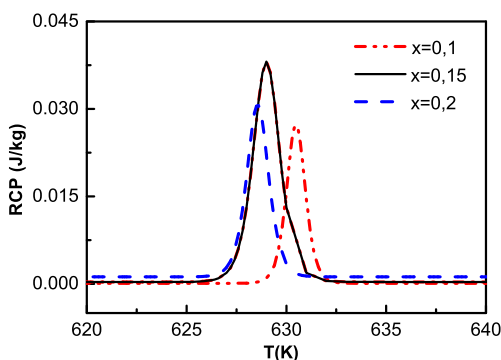


Fig. 7 Temperature dependences of calculated values of the relative cooling power (RCP) for the $\text{BiFe}_{1-x}\text{Zn}_x\text{O}_3$ ceramic samples in a magnetic field of 6 T

Table 2 Calculated values of magnetocaloric characteristics for the $\text{BiFe}_{1-x}\text{Zn}_x\text{O}_3$ ceramic samples in a magnetic field of 6 T

x	$-\Delta S_{\max}$ (J/kg·K)	δT_{FWHM} (K)	$\Delta C_{p,H(\max)}$ (J/kg·K)	RCP_{\max} (J/kg)
0.10	0.006	4.90	0.27	0.027
0.15	0.006	6.92	0.27	0.038
0.20	0.005	5.65	0.40	0.022

with increase in x , the Neel temperature decreases and the values of δT_{FWHM} and RCP increase passing through the relative maxima at $x = 0.15$. The magnetic transition occurs in narrow temperature ranges. With the increase in the degree of bismuth substitution, the temperature, corresponding to the maximum values of the calculated characteristics, monotonically decreases. The variation of temperature values, corresponding to the maximum values of RCP and ΔS_{\max} , is in the range from 630.5 K ($x = 0.10$) to 628.6 K ($x = 0.20$). This range for the $\Delta C_{p,H}$ contribution varies from 630.7 to 629.1 K. The values of the ΔS_{\max} and $\Delta C_{p,H}$ contributions almost do not depend on the concentration of zinc cations.

With the increase in the content of Zn^{2+} cations, the average effective radius of cation in the B sublattice decreases. The decrease in Neel temperature with increase in the concentration of zinc cations can be explained by the fact that the values of Fe–O–Zn angles also change, and consequently, the degree of distortion of the crystal lattice increases, which leads to a change in the conditions and intensity of the indirect (through oxygen anions) magnetic interaction of iron cations of the Dzyaloshinsky-Moriya type. At the same time, since the magnetoactive cations of iron are replaced by diamagnetic cations of zinc, the absolute magnitudes of the specific magnetizations decrease. The monotonic decrease in the values of Neel temperatures can be related to the decrease in the valence bond angles of Fe–O–Fe.

4 Conclusions

On the basis of obtained experimental results of magnetic measurements, the study of magnetocaloric properties of multiferroic BFZO ceramics was carried out. For prediction of MCE around the antiferromagnetic phase transition temperature, the theoretical model was applied. Results of the investigation confirmed the presence of the maximum of magnetocaloric effect in the vicinity of antiferromagnetic Neel temperature. Maximum value of MCE was obtained for sample with concentration $x = 0.15$ and related with higher values of magnetization in comparison with another compositions. The concentration dependences of maximum

magnitudes of the entropy, relative cooling power, and magnetic contributions to heat capacity of the samples indicate that the practical use of magnetocaloric effect in BFZO at the temperatures above room temperature is hardly suitable. The obtained results can be used for prediction and modeling of MCE in multiferroic materials.

Acknowledgements The authors are grateful to Dr. M. Guseinov (Amirkhanov Institute of Physics Dagestan Scientific Center, Russian Academy of Sciences) and Dr. K. Chichay (Immanuel Kant Baltic Federal University) for the help in measurements.

Funding Information This work was partially supported by projects “Phase transitions, magnetotransport, magnetocaloric, magnetoelectric phenomena in strongly correlated electron systems” (No. 0203-2016-0009) at the Institute of Physics of Dagestan Scientific Center of Russian Academy of Sciences and 5 top 100 Russian Academic Excellence Project at the Immanuel Kant Baltic Federal University. The work was partially supported by the Ukrainian State Foundation for Basic Research, project F71/46-2017.

References

1. Aizu, K.: *Phys. Rev. B.* **2**, 754 (1970)
2. Schmid, H.: *Ferroelectrics* **162**, 317 (1994)
3. Manosa, L., Gonzalez-Alonso, D., Planes, A., Bonnot, E., Barrio, M., Tamarit, J.L., Aksoy, S., Acet, M.: *Nat. Mater.* **9**, 478 (2010)
4. Planes, A., Castan, T., Saxena, A.: *Philos. Mag.* **94**, 1893 (2014)
5. Fahler, S., Robler, U.K., Kastner, O., Eckert, J., Eggeler, G., Emmerich, H., Entel, P., Muller, S., Quandt, E., Albe, K.: *Adv. Eng. Mater.* **14**, 10 (2012)
6. Flerov, I., Mikhaleva, E., Gorev, M., Kartashev, A.: *Phys. Solid State* **57**, 429 (2015)
7. Kumar, A., Yadav, K.: *J. Appl. Phys.* **116**, 083907 (2014)
8. Lisenkov, S., Mani, B., Chang, C.M., Almand, J., Ponomareva, I.: *Phys. Rev. B* **87**, 224101 (2013)
9. Liu, Y., Infante, I.C., Lou, X., Lupascu, D.C., Dkhil, B.: *Appl. Phys. Lett.* **104**, 012907 (2014)
10. Starkov, A., Starkov, I.: *J. Exp. Theor. Phys.* **119**, 258 (2014)
11. Starkov, I.A., Starkov, A.S.: *Int. J. Solids Struct.* **100**, 187 (2016)
12. Teague, J.R., Gerson, R., James, W.J.: *Sol. Stat. Commun.* **8**, 1073 (1970)
13. Fischer, P., Polomska, M.: *J. Phys. C: Sol. Stat.* **13**, 1931 (1980)
14. Starkov, I., Starkov, A.: *Int. J. Refrig.* **37**, 249 (2014)
15. Zheng, G.-P., Sarir, U., Zheng, X., Yang, J.: *J. Alloys Compd.* **663**, 249 (2016)
16. Chaudhari, Y.A., Singh, A., Abuassaj, E.M., Chatterjee, R., Bendre, S.T.: *J. Alloys Compd.* **518**, 51 (2012)
17. Amirov, A.A., Kamilov, I.K., Yusupov, D.M., Reznichenko, L.A., Razumovskaya, O.N., Verbenko, I.A.: *Phys. Procedia* **75**, 10 (2015)
18. Kozakov, A.T., Kochur, A.G., Torgashev, V.I., Googlev, K.A., Kubrin, S.P., Trotsenko, V.G., Bush, A.A., Nikolskii, A.V.: *J. Alloys Compd.* **664**, 392 (2016)
19. Prado-Gonjal, J., Ávila, D., Villafuerte-Castrejón, M.E., González-García, F., Fuentes, L., Gómez, R.W., Pérez-Mazariego, J.L., Marquina, V., Morán, E.: *Solid State Sci.* **13**, 2030 (2011)
20. Hamad, M.A.: *Phase Transit.* **85**, 106 (2012)
21. M'nassri, R., Cheikhrouhou, A.: *J. Supercond. Nov. Magn.* **27**, 421 (2014)
22. Franco, V., Conde, A., Kiss, L.F.: *J. Appl. Phys.* **104**, 033903 (2008)
23. Phan, M.H., Yu, S.C.: *J. Magn. Magn. Mater.* **308**, 325 (2007)
24. Foldeaki, M., Chahine, R., Bose, T.K.: *J. Appl. Phys.* **77**, 3528 (1995)